



Cite this: *Phys. Chem. Chem. Phys.*,  
2018, 20, 20427

## Fluctuations of random walks in critical random environments

Yousof Mardoukhi,<sup>a</sup> Jae-Hyung Jeon,<sup>bc</sup> Aleksei V. Chechkin<sup>ad</sup> and Ralf Metzler<sup>id</sup>\*<sup>a</sup>

Percolation networks have been widely used in the description of porous media but are now found to be relevant to understand the motion of particles in cellular membranes or the nucleus of biological cells. Random walks on the infinite cluster at criticality of a percolation network are asymptotically ergodic. On any finite size cluster of the network stationarity is reached at finite times, depending on the cluster's size. Despite of this we here demonstrate by combination of analytical calculations and simulations that at criticality the disorder and cluster size average of the ensemble of clusters leads to a non-vanishing variance of the time averaged mean squared displacement, regardless of the measurement time. Fluctuations of this relevant experimental quantity due to the disorder average of such ensembles are thus persistent and non-negligible. The relevance of our results for single particle tracking analysis in complex and biological systems is discussed.

Received 20th May 2018,  
Accepted 19th July 2018

DOI: 10.1039/c8cp03212b

rsc.li/pccp

### 1. Introduction

Fractals gained immense popularity after Benoît Mandelbrot published his famous book *The fractal geometry of nature* which contains the by now iconic phrase “Clouds are not spheres, mountains are not cones, coastlines are not circles, and bark is not smooth, nor does lightning travel in a straight line”.<sup>1</sup> Indeed, natural objects in most cases cannot be characterised by a single scale but exhibit some sort of statistical self-similarity. For instance, the length of the coastlines of Britain or Norway varies as function of the applied yard stick, and similar features appear on different scales.<sup>1–3</sup>

Yet self-similarity is typically not sufficient to describe natural objects, either. Thus, mathematical (deterministic) fractals such as the well known Cantor set (or the multi-dimensional Cantor dust),<sup>4</sup> the von Koch snowflake,<sup>5</sup> or the Sierpiński gasket<sup>6</sup> are composed of exact iterations of an identical operation, such as the removal of the middle third of a line segment for the Cantor set. The resulting symmetries appear artificial. To combine self-similarity—on a statistical, not deterministic sense—with the non-perfect structures of mountains or coastlines, random fractals have been considered such as landscapes created by (fractional) Brownian trajectories.<sup>1,2</sup>

A breakthrough in statistical physics was the conception of percolation theory originally proposed by Broadbent and Hammersley.<sup>7</sup> In the language of site percolation, imagine that

on a discrete lattice each lattice site is occupied with probability  $p$  and left vacant otherwise. Nearest occupied (or vacant) neighbours on the lattice are considered to be connected, and each set of connected occupied (or vacant) lattice sites forms an occupied (or vacant) cluster. Here we will focus on open clusters  $\mathcal{C}$  formed by vacant sites, their size being denoted by  $|\mathcal{C}|$ . Statistical analysis shows that there exists a critical percolation probability  $p_c$  at which an open cluster arises which spans the entire lattice, the incipient infinite percolation cluster. If we place a particle randomly on a vacant lattice site, it will either be on the infinite cluster or on any of the finite-sized open clusters. Notably, at criticality the percolation network is a random fractal whose Hausdorff dimension can be calculated for a number of lattice types and dimensions by renormalisation arguments.<sup>2,8</sup> On a square lattice, the centre of the current study, the fractal dimension is  $d_f = 91/48$ , while the distribution of cluster sizes is characterised by the Fisher exponent  $\tau = 187/91$ .<sup>9</sup> An example for a finite open cluster is shown in Fig. 1.

A random walker moving on fractal open clusters at criticality continuously encounters dead ends and has to pass through bottlenecks, a situation that was pictorially characterised as the motion of “an ant in a labyrinth” by de Gennes.<sup>10</sup> In fact the fractal nature of the geometric constraints effect a power-law growth of the mean squared displacement (MSD)

$$\langle |\mathbf{r}(t) - \mathbf{r}(0)|^2 \rangle \simeq t^\alpha, \quad (1)$$

on the infinite cluster, where the scaling exponent can be expressed as  $\alpha = 2/d_w$  in terms of the fractal walk dimension  $d_w \approx 2.87$  on the square lattice.<sup>9</sup> The resulting value  $\alpha \approx 0.70$  demonstrates that the motion of the random walker is subdiffusive,<sup>11</sup> that is, indicating less efficient spreading than on a fully accessible Euclidean lattice, for which  $d_w = 2$  and thus the diffusion is normal,  $\alpha = 1$ .

<sup>a</sup> Institute of Physics and Astronomy, University of Potsdam, 14476 Potsdam-Golm, Germany. E-mail: rmetzler@uni-potsdam.de

<sup>b</sup> School of Physics, Korea Institute for Advanced Study, Seoul 02455, Republic of Korea

<sup>c</sup> Department of Physics, Pohang University of Science and Technology, Pohang 37673, Republic of Korea

<sup>d</sup> Akhiezer Institute for Theoretical Physics, Kharkov 61108, Ukraine

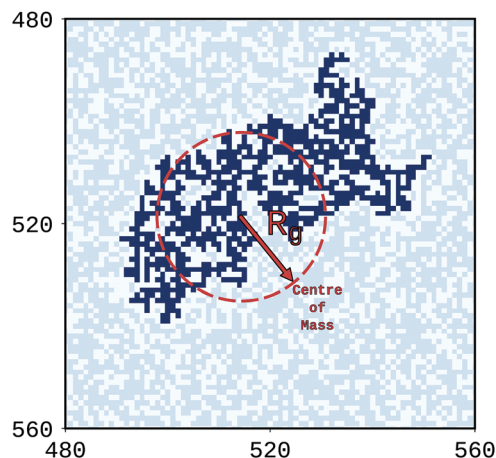


**Fig. 1** Finite open cluster of size  $|C| = 793$  represented by Oxford blue on a square lattice at criticality. The arrow starts at the centre of mass of the cluster, and its tip defines a circle whose radius is the radius of gyration  $R_g$  of the open cluster. The co-ordinates show the lattice points of the entire network. Sky blue sites represent other vacant lattice sites, the powder blue (off-white) sites are occupied. Note that we consider the motion of particles on connected vacant lattice sites.

The emerging subdiffusion on a critical percolation network on a square lattice was demonstrated experimentally by field gradient NMR methods of water diffusion in thin plastic sheets, into which the cluster geometry was milled.<sup>12,13</sup>

Percolation networks have classically been used as model systems for porous media.<sup>8,14,15</sup> More recently single particle tracking experiments monitoring the motion of protein channels in membranes of living biological cells showed that these particles were confined to move on a fractal, percolation-like support.<sup>16</sup> From a modelling perspective percolation networks have been employed to characterise the diffusive motion of, typically submicron, tracer particles in the crowded cytoplasm of biological cells or in their membranes.<sup>17–20</sup> We also mention applications of studies on adaptive growth and branching of plants in heterogeneous environments<sup>21</sup> and to labour division in economic contexts.<sup>22</sup> While the majority of studies focuses on the motion on the infinite cluster, only relatively few consider the impact of the co-existing finite sized clusters.<sup>8,23</sup>

To analyse particle tracking experiments or simulations involving percolation networks at criticality, it is important to have available precise analytical tools to quantify the observed dynamics. Typically, single particle trajectories are evaluated in terms of time averaged mean squared displacements (TAMSDs),<sup>24–28</sup> see eqn (3) below. The prime question in this context is whether the information encoded in the TAMSD is equivalent to that of the ensemble MSD (1) or not. This question is related to ergodicity in the weaker sense that sufficiently long time averages of a physical quantity are equivalent to the corresponding ensemble average.<sup>24,25,29</sup>

Non-stationary anomalous diffusion processes such as the famed continuous time random walk, in which successive motion events are interspersed with immobile periods with scale-free distribution of waiting times<sup>15,25,30</sup> or heterogeneous diffusion processes with space-dependent mobility<sup>31–33</sup> are inherently non-ergodic and exhibit fundamental differences

between the MSD and TAMSD,<sup>24,25,34–36</sup> which was indeed shown experimentally.<sup>16,37–39</sup> They also exhibit pronounced ageing effects.<sup>16,25,38–43</sup> Conversely, processes dominated by viscoelastic effects driven by long-range correlated fractional Gaussian noise—stationary in their increments—are ergodic and do not age.<sup>16,37,44–48</sup>

Random walks on the infinite percolation cluster were demonstrated to be ergodic.<sup>49,50</sup> Moreover, it was shown that the increment correlation function for diffusion on a critical square percolation network is indistinguishable from the one for (overdamped) viscoelastic diffusion.<sup>49,50</sup> In our previous analysis<sup>51</sup> we went one step further and took all, incipient infinite and the full ensemble of finite clusters into account. We demonstrated that below, above, as well as at the percolation threshold the average over TAMSDs over a large set of particles indeed converged to the MSD. However, we also showed that due to the random seeding, the TAMSDs of those particles diffusing on finite clusters were eventually dominated by the finite size, and thus intrinsically different from each other. As a particle seeded on a finite cluster cannot jump to another cluster this is some form of strong ergodicity breaking in the sense that the phase space is topologically disconnected. Only the disorder average including the full ensemble of geometries restores ergodicity on this level. In particular, we obtained that even after both ensemble and disorder averages were taken, the amplitude fluctuations of the TAMSD quantified by the ergodicity breaking parameter were characterised by a finite variance.

Here we further analyse the fluctuations of the TAMSD on a critical percolation network. We carefully separate the behaviour of the trajectory on a single cluster, from that of the disorder averaged dynamics. In what follows, after defining the fundamental quantities of MSD and TAMSD on a given topology we conjecture the analogy of the current problem with the Ornstein–Uhlenbeck process. This formal correspondence is then used to calculate the ensemble averages of the MSD and TAMSD. In a further step we then take the disorder average, based on which we quantify the amplitude fluctuations of the TAMSD. Our results are put into perspective in the Discussion section, particular, with respect to single particle tracking analysis in complex and biological systems, before collecting some details in the Methods section.

## II. Results

### A. Random walks and percolation

For an ensemble of random walkers on a given open cluster  $C$  of the percolation network the MSD is defined as

$$\langle \mathbf{r}_C^2(t) \rangle = \langle |\mathbf{r}(t) - \mathbf{r}(0)|^2 \rangle, \quad (2)$$

where the angular brackets indicate an ensemble average over random walks sampled over that specific cluster. The TAMSD for the same ensemble of random walks on this cluster is defined as<sup>24,25,34</sup>

$$\langle \overline{\delta_C^2(\Delta)} \rangle = \frac{1}{T - \Delta} \int_0^{T-\Delta} \langle |\mathbf{r}(t + \Delta) - \mathbf{r}(t)|^2 \rangle dt, \quad (3)$$

where  $T$  is the overall length of the measured time series and  $\Delta$  is called the lag time.

An essential complication for evaluating these quantities is the lack of full knowledge of the probability density function for diffusion on random fractals. Despite scaling arguments based on the radial distribution of the mass of the fractal support<sup>52</sup> or attempts to reproduce the scaling behaviour of the probability density function in terms of fractional diffusion equations,<sup>53,54</sup> this question has remained elusive. A more promising approach is based on dynamical scaling theories, which address questions on the scaling behaviour of statistical quantities of random walks averaged over all clusters, relating them to the geometrical exponents of percolation clusters.<sup>9,55</sup> This is basically the approach chosen here to study random walk processes for the full ensemble of clusters at criticality.

Assume an ensemble of open clusters onto which random walkers parachute. Randomly, they may either land on the incipient infinite cluster or on a finite-sized open cluster. Denote the linear size explored by a random walker after infinitely many steps by  $R_\infty$ , then the MSD assumes the value,<sup>55,56</sup>

$$\frac{R_\infty^2 - \langle \mathbf{r}_c^2(t) \rangle}{R_\infty^2} \sim \exp\left(-\left[\frac{t}{\chi}\right]^w\right). \quad (4)$$

Here  $w$  is a positive definite exponent which depends on the underlying topology only, and  $\chi$  is a characteristic time needed by the random walkers such that they will eventually feel the effective linear size of the underlying cluster  $\mathcal{C}$ .<sup>55</sup> Note that when the underlying cluster tends to be the incipient infinite cluster, then  $\chi \rightarrow \infty$  and one observes that  $\langle \mathbf{r}_c^2(t) \rangle \simeq t^w$ .

In their work Mitescu *et al.* originally assumed  $w$  to be unity,<sup>57</sup> but later simulation studies of Fassnacht and Pandey revealed a value smaller than unity in three dimension.<sup>58,59</sup> While the general form of eqn (4) was qualitatively confirmed by simulations, numerical analyses performed by Jacobs *et al.*, based on transition probability matrix formalism, estimated  $w$  to be  $2/d_w$ .<sup>56</sup>

For a finite size cluster  $\mathcal{C}$  it is evident that the MSD or TAMSD will eventually reach a saturation plateau, the time needed to reach the plateau depending on the size of the cluster. For such a cluster, at saturation the MSD, averaged over equilibrium initial positions with equal weight  $1/|\mathcal{C}|$  is twice the squared of the radius of gyration  $R_g$  of that cluster.<sup>60,61</sup> Hence we rewrite eqn (4) in the form

$$\langle \mathbf{r}_c^2(t) \rangle = 2R_g^2 \left(1 - \exp\left[-\left(\frac{t}{\chi}\right)^{2/d_w}\right]\right). \quad (5)$$

Here the subscript eq. refers to the equilibrium initial condition. Due to the time invariance at equilibrium the TAMSD  $\langle \overline{\delta c^2(\Delta)} \rangle$  is identical to  $\langle \mathbf{r}_c^2(t) \rangle$ , with time  $t$  replaced by lag time  $\Delta$ ,

$$\langle \overline{\delta c^2(\Delta)} \rangle = 2R_g^2 \left(1 - \exp\left[-\left(\frac{\Delta}{\chi}\right)^{2/d_w}\right]\right). \quad (6)$$

**Analogy between Ornstein–Uhlenbeck process and random walks on finite size open clusters.** However, what happens when the initial seeding of random walkers is different from

the above-assumed equilibrium initial condition? This situation will be of relevance for many real systems whose experimental preparation coincides with the start of the measurement at  $t = 0$ . For instance, in a porous matrix a single colloidal particle is released at a specific point on the cluster, a drop of a tracer chemical trickles down into a soil aquifer from above, or a neuronal synapse sends a signal pulse in a neural network. In our simulations delineated below we adopt this non-equilibrium stance and always seed the random walker at the centre of the lattice. We therefore need to seek a new set of equations for the MSD and TAMSD to address non-equilibrium initial conditions, the purpose of this section. We achieve this by using the analogy between the generic Ornstein–Uhlenbeck processes and random walks on finite size open clusters based on the universal form of eqn (4).

As discussed earlier the precise form of the probability density function for diffusion on a random fractal is unknown. That makes it arduous to approach random walk processes on finite size open clusters by standard methods such as solving the stochastic differential equation associated to the processes and its corresponding Fokker–Planck equation with appropriate boundary conditions, or to employ path integral methods. Looking at eqn (4) one may note that such a form for the MSD for  $w = 1$  corresponds to the relaxation dynamics of a random walker in the Ornstein–Uhlenbeck process (diffusion in an harmonic potential).<sup>62,63</sup>

As addressed in ref. 63 the Langevin equation for the Ornstein–Uhlenbeck process in two dimensions with positive parameters  $\chi$  and  $\sigma$  and a randomly distributed initial condition  $\mathbf{r}_0$  in the presence of the white and zero-mean Gaussian noise  $\xi(t)$  is given by

$$\frac{d\mathbf{r}}{dt} = -\frac{\mathbf{r}}{\chi} + \sigma\xi(t), \quad \langle \xi_i(t_1)\xi_j(t_2) \rangle = \delta_{ij}\delta(t_1 - t_2); \quad i, j \in \{x, y\}. \quad (7)$$

For such processes the MSD and TAMSD are found to be<sup>63</sup>

$$\langle \mathbf{r}_{OU}^2(t) \rangle = \langle \mathbf{r}_0^2 \rangle \left(1 - \exp\left[-\left(\frac{t}{\chi}\right)\right]\right)^2 + \chi\sigma^2 \left(1 - \exp\left[-2\left(\frac{t}{\chi}\right)\right]\right), \quad (8a)$$

$$\begin{aligned} \langle \overline{\delta_{OU}^2(\Delta)} \rangle &= 2\chi\sigma^2 \left(1 - \exp\left[-\left(\frac{\Delta}{\chi}\right)\right]\right) + (\langle \mathbf{r}_0^2 \rangle - \chi\sigma^2) \\ &\times \left(1 - \exp\left[-\left(\frac{\Delta}{\chi}\right)\right]\right)^2 \left(\frac{1 - \exp\left[-2\left(\frac{T-\Delta}{\chi}\right)\right]}{2\left(\frac{T-\Delta}{\chi}\right)}\right). \end{aligned} \quad (8b)$$

To identify the similarity between Ornstein–Uhlenbeck processes and random walks on finite size open clusters, it is sufficient to consider the equilibrium initial condition for  $\mathbf{r}_0$ , which implies  $\langle \mathbf{r}_0^2 \rangle = \chi\sigma^2$ .<sup>63</sup> Such a condition then yields

$$\langle \mathbf{r}_{OU}^2(t) \rangle_{\text{eq.}} = 2\chi\sigma^2 \left(1 - \exp\left[-\left(\frac{t}{\chi}\right)\right]\right), \quad (9a)$$

$$\langle \overline{\delta_{OU}^2(\Delta)} \rangle_{\text{eq.}} = 2\chi\sigma^2 \left( 1 - \exp \left[ - \left( \frac{\Delta}{\chi} \right) \right] \right). \quad (9b)$$

One then can immediately relate this set of equations to expressions (5) and (6). Additionally, eqn (8a) and (8b) provide a clear clue to conjecture a new set of relations for the MSD and TAMSD for random walks in finite random environments when the equilibrium initial condition is not satisfied. Thus assume that a random walk on a cluster  $\mathcal{C}$  with gyration radius  $R_g$  and characteristic time  $\chi$  is analogous to an Ornstein–Uhlenbeck process with parameters  $\chi$  and  $\sigma$ , in which  $R_g^2 = \chi\sigma^2$  and time  $t$  is rescaled as  $t^{2/d_w}$ . Thus we arrive at the following expressions,

$$\langle \mathbf{r}_C^2(t) \rangle = \langle \mathbf{r}_0^2 \rangle \left( 1 - \exp \left[ - \left( \frac{t}{\chi} \right)^{2/d_w} \right] \right)^2 + R_g^2 \left( 1 - \exp \left[ - 2 \left( \frac{t}{\chi} \right)^{2/d_w} \right] \right), \quad (10a)$$

$$\begin{aligned} \langle \overline{\delta_C^2(\Delta)} \rangle &= 2R_g^2 \left( 1 - \exp \left[ - \left( \frac{\Delta}{\chi} \right)^{2/d_w} \right] \right) \\ &+ (\langle \mathbf{r}_0^2 \rangle - R_g^2) \left( 1 - \exp \left[ - \left( \frac{\Delta}{\chi} \right)^{2/d_w} \right] \right)^2 \\ &\times \left( \frac{1 - \exp \left[ - 2 \left( \frac{T - \Delta}{\chi} \right)^{2/d_w} \right]}{2 \left( \frac{T - \Delta}{\chi} \right)^{2/d_w}} \right). \end{aligned} \quad (10b)$$

We now show that expressions (10), deduced from analogy with the Ornstein–Uhlenbeck process, are consistent with the known limiting behaviours of both the MSD and the TAMSD. Below we will also demonstrate good agreement with simulations results. In the limit of short times  $t \ll \chi$  we recover the expected free anomalous diffusion behaviour  $\langle \mathbf{r}_C^2(t) \rangle \simeq t^{2/d_w}$  of the MSD, while for  $\Delta \ll \chi$  the TAMSD becomes  $\langle \overline{\delta_C^2(\Delta)} \rangle \simeq \Delta^{2/d_w}$ . Conversely, in the long time limit  $t, T \rightarrow \infty$ , eqn (10) have the following asymptotes,

$$\lim_{t \rightarrow \infty} \langle \mathbf{r}_C^2(t) \rangle = \langle \mathbf{r}_0^2 \rangle + R_g^2 \quad (11a)$$

$$\lim_{T \rightarrow \infty} \langle \overline{\delta_C^2(\Delta)} \rangle = \begin{cases} 2R_g^2, & \text{if } \chi < \Delta \ll T \\ \langle \mathbf{r}_0^2 \rangle + R_g^2, & \text{if } \Delta \rightarrow T \end{cases}. \quad (11b)$$

This limit indeed produces the expected values.

These asymptotes can alternatively be derived by invoking the generic definition of the MSD and TAMSD given by relations (2) and (3). To demonstrate this for the TAMSD consider a finite size open cluster  $\mathcal{C}$ . According to eqn (3) for lag times  $\Delta \rightarrow T$  the TAMSD saturates at a certain level, assuming that  $\chi \ll T$ , which guarantees

that the random walker would have enough time to visit each site of the cluster equally. Then

$$\begin{aligned} \lim_{\Delta \rightarrow T} \langle \overline{\delta_C^2(\Delta)} \rangle &= \lim_{\Delta \rightarrow T} \frac{1}{T - \Delta} \int_0^{T - \Delta} \langle |\mathbf{r}(t + \Delta) - \mathbf{r}(t)|^2 \rangle dt \\ &= \langle |\mathbf{r}(T) - \mathbf{r}(0)|^2 \rangle. \end{aligned}$$

In the centre of mass co-ordinate system, used here for convenience,

$$\langle |\mathbf{r}(T) - \mathbf{r}(0)|^2 \rangle = \langle |\mathbf{r}(T) - \mathbf{r}_{C,\text{cm}} + \mathbf{r}_{C,\text{cm}} - \mathbf{r}(0)|^2 \rangle, \quad (12)$$

where  $\mathbf{r}_{C,\text{cm}} = \frac{1}{\|\mathcal{C}\|} \sum_{s=1}^{\|\mathcal{C}\|} \mathbf{r}_{C,s}$  is the centre of mass of the finite size open cluster. Here  $\mathbf{r}_{C,s}$  represents the spatial position of site  $s$  in the cluster  $\mathcal{C}$ . In the limit  $N \rightarrow \infty$ , where  $N$  is the number of random walk processes on a given cluster, due to the finite cluster size visiting any site  $s_j \in \mathcal{C}$  becomes equally probable. Thus  $\mathbf{r}(T)$  would be any  $\mathbf{r}_{C,s}$ , where the probability of visitation is  $1/\|\mathcal{C}\|$ . Therefore the ensemble average would be equivalent to taking an average over different cluster sites. Hence,

$$\begin{aligned} \lim_{\Delta \rightarrow T} \langle \overline{\delta_C^2(\Delta)} \rangle &= \frac{1}{\|\mathcal{C}\|} \sum_{s=1}^{\|\mathcal{C}\|} [|\mathbf{r}_{C,s} - \mathbf{r}_{C,\text{cm}}|^2 + |\mathbf{r}_{C,\text{cm}} - \mathbf{r}(0)|^2 \\ &+ 2(\mathbf{r}_{C,s} - \mathbf{r}_{C,\text{cm}}) \cdot (\mathbf{r}_{C,\text{cm}} - \mathbf{r}(0))]. \end{aligned} \quad (13)$$

In the equation above, the square root of the first term is simply the definition of the radius of gyration  $R_g$  for a given cluster  $\mathcal{C}$  and the third term vanishes. This yields

$$\langle \overline{\delta_C^2(\Delta)} \rangle = R_g^2 + \langle |\mathbf{r}_{C,\text{cm}} - \mathbf{r}(0)|^2 \rangle, \quad \Delta \rightarrow T, \quad (14)$$

where  $|\mathbf{r}(0) - \mathbf{r}_{C,\text{cm}}|^2$  (equivalent to  $\mathbf{r}_0^2$  in eqn (11a)) is a random variable which depends on the initial position of the random walkers.

In the current form of eqn (10a) and (10b) the dependence of  $\chi$  and  $R_g$  on  $\mathcal{C}$  is not evident. To find the relation between these quantities, dynamical scaling theory is exploited. The time which is required by a random walker to reach the linear length scale of a cluster  $\mathcal{C}$  can be approximated as follows: on length scales smaller than  $R_g$  the boundaries of the underlying finite cluster can not yet be reached by the walker, and thus  $\langle \mathbf{r}_C^2(t) \rangle = D t^{2/d_w}$ , where  $D$  is the anomalous diffusion coefficient.<sup>8,55</sup> Therefore the typical time scale  $\chi$  required for a random walker to reach a length scale comparable to  $\sqrt{2R_g^2}$ , scales as  $\chi = \left( \frac{2}{D} \right)^{d_w/2} R_g^{d_w}$ . From this scaling relation and the scaling relation for the mass distribution of fractal objects,  $R_g^{d_f} = h^{d_f} \|\mathcal{C}\|$  (where  $h$  is a dimensional constant),<sup>9</sup> on the time

scale  $\chi$  one attains  $\chi^{2/d_w} = \frac{2h^2}{D} \|\mathcal{C}\|^{2/d_f}$ . Including this relation into eqn (10a) and (10b), we obtain the modified relations

$$\langle \mathbf{r}_c^2(t) \rangle = \langle \mathbf{r}_0^2 \rangle \left( 1 - \exp \left[ -\frac{\mathcal{D} t^{2/d_w}}{\|\mathcal{C}\|^{2/d_f}} \right] \right)^2 + h^2 \|\mathcal{C}\|^{2/d_f} \left( 1 - \exp \left[ -\frac{2\mathcal{D} t^{2/d_w}}{\|\mathcal{C}\|^{2/d_f}} \right] \right), \quad (15a)$$

$$\begin{aligned} \langle \overline{\delta c^2(\Delta)} \rangle &= 2h^2 \|\mathcal{C}\|^{2/d_f} \left( 1 - \exp \left[ -\frac{\mathcal{D} \Delta^{2/d_w}}{\|\mathcal{C}\|^{2/d_f}} \right] \right) \\ &+ \left( \langle \mathbf{r}_0^2 \rangle - h^2 \|\mathcal{C}\|^{2/d_f} \right) \left( 1 - \exp \left[ -\frac{\mathcal{D} \Delta^{2/d_w}}{\|\mathcal{C}\|^{2/d_f}} \right] \right)^2 \\ &\times \left( \frac{1 - \exp \left[ -2\mathcal{D} \frac{(T-\Delta)^{2/d_w}}{\|\mathcal{C}\|^{2/d_f}} \right]}{2\mathcal{D} \frac{(T-\Delta)^{2/d_w}}{\|\mathcal{C}\|^{2/d_f}}} \right). \end{aligned} \quad (15b)$$

Here we introduced  $\mathcal{D} = D/(2h^2)$ . For validation of this approach based on the analogy with the Ornstein–Uhlenbeck process, by extensive Monte Carlo simulations we refer to Fig. 5.

## B. Disorder average: anisotropy and cluster size average

In an ensemble of open clusters, it is not only the size of the clusters that matters but also their topological structure and the distribution of their mass around their centre of mass. These two factors together define the disorder average. Indeed, averaging over the anisotropy of same-sized open clusters yields a result, which is equivalent to averaging over the randomly distributed initial position of the random walks, producing an equilibrium situation. This observation simplifies the rest of the calculations regarding the cluster size average over the ensemble of finite size open clusters.

**Anisotropy average of the TAMSD over all possible same-sized clusters.** We take a disorder average of the TAMSD in two steps. First we average over all possible clusters of the same size, then we average over the distribution of cluster sizes. In the first step we note that averaging over  $\langle \mathbf{r}_0^2 \rangle$  yields exactly  $R_g^2$ , which is intuitively clear (see also the Methods section). The TAMSD (15b) after anisotropy averaging returns expression (6) corresponding to equilibrium initial conditions.

It is interesting to observe that due to this averaging the  $T$  dependence of  $\langle \overline{\delta c^2(\Delta)} \rangle$  disappears. Indeed, this is not surprising as the average over all clusters of the same size is equivalent to the averaging over the equilibrium initial condition corresponding to the specific system. To clarify the equivalence between these two, recall that the equilibrium initial condition for a cluster  $\mathcal{C}$  is realised once the random walk process is initiated randomly with equal weight  $1/\|\mathcal{C}\|$  at any possible site in  $\mathcal{C}$ . Now, instead of choosing the initial position randomly, shift the underlying lattice and choose randomly the centre of the lattice within the cluster  $\mathcal{C}$  while keeping the initial position of the random walk at the centre of the lattice. Since the lattice remains the same under translational transformations the new configuration is equal to

realisations of different clusters with the same size and shape. Therefore one observes that randomly choosing the initial positions of random walkers is equivalent to randomly choosing the centre of the lattice within the cluster by shifting the underlying lattice. In the Methods section a more formal proof is provided for the anisotropy average over clusters of size three. There it will be demonstrated further that in the simulations this claim also holds true.

**Cluster size average of  $\langle \overline{\delta c^2(\Delta)} \rangle$ .** For the ensemble of finite size open clusters  $\{\mathcal{C}\}$  the cluster size average of  $\langle \overline{\delta c^2(\Delta)} \rangle$  (eqn (6)) is given by

$$\langle \overline{\delta c^2(\Delta)} \rangle = \sum_{\{\mathcal{C}\}} \mathcal{P}(\|\mathcal{C}\|) \langle \overline{\delta c^2(\Delta)} \rangle, \quad (16)$$

where  $\mathcal{P}(\|\mathcal{C}\|)$  is the probability for a random walker to land on cluster  $\mathcal{C}$ . This probability is simply given by the probability of the appearance of such a cluster in a specific realisation of the underlying percolation network, multiplied by the probability that the centre of the lattice would belong to this cluster. The probability distribution for the cluster  $\mathcal{C}$  to appear in a specific lattice realisation at the critical percolation density is  $\simeq \|\mathcal{C}\|^{-\tau}$ , where  $\tau$  is a scaling exponent called the Fisher exponent.<sup>9</sup> Therefore, the probability that the centre of the lattice would belong to this cluster scales as  $\|\mathcal{C}\|^{1-\tau}$ ,<sup>8</sup> such that

$$\langle \overline{\delta c^2(\Delta)} \rangle = \Xi \sum_{\|\mathcal{C}\|=1}^{\infty} \langle \overline{\delta c^2(\Delta)} \rangle \|\mathcal{C}\|^{1-\tau}. \quad (17)$$

Here  $\Xi$  is a normalisation constant. Taking the continuum limit of the summation (see ref. 9, eqn (21)) and substituting relation (6), the evaluation of the integral yields the cluster size average of  $\langle \overline{\delta c^2(\Delta)} \rangle$ ,

$$\langle \overline{\delta c^2(\Delta)} \rangle = \Xi \int_{\|\mathcal{C}\|}^{\infty} 2h^2 \left( 1 - \exp \left[ -\frac{\mathcal{D} \Delta^{2/d_w}}{\|\mathcal{C}\|^{2/d_f}} \right] \right) \|\mathcal{C}\|^{2/d_f+1-\tau} d\|\mathcal{C}\|, \quad (18)$$

where  $\|\mathcal{C}\|$  is the smallest cluster in  $\{\mathcal{C}\}$ . Substituting the argument of the exponential function we evaluate the integral, producing

$$\begin{aligned} \langle \overline{\delta c^2(\Delta)} \rangle &= (\tau-2) \|\mathcal{C}\|^{\tau-2} \left\{ -\frac{2d_f h^2}{2+d_f(2-\tau)} \|\mathcal{C}\|^{2d_f+2-\tau} \right. \\ &\left. - d_f h^2 \mathcal{D}^{1+\frac{d_f}{2}(2-\tau)} \gamma \left( -1 - \frac{d_f}{2}(2-\tau), \frac{\mathcal{D} \Delta^{2/d_w}}{\|\mathcal{C}\|^{2/d_f}} \right) \Delta^{\frac{2+d_f(2-\tau)}{d_w}} \right\}, \end{aligned} \quad (19)$$

where  $\gamma(a,x)$  represents the lower incomplete gamma function.

**Normalised variance of  $\langle \overline{\delta c^2(\Delta)} \rangle$ .** To evaluate the variance of the TAMSD we need to evaluate the cluster size average of  $\langle \overline{\delta c^2(\Delta)} \rangle^2$ . After following the same procedure carried out for

$\langle \overline{\delta c^2(\Delta)} \rangle$ , we find

$$\begin{aligned} \langle \overline{\delta c^2(\Delta)} \rangle^2 &= (\tau - 2) \|c\|^{\tau-2} \left\{ \frac{4d_f h^4 \|c\|^{4d_f+2-\tau}}{4 + d_f(2-\tau)} - 4d_f h^4 \mathcal{D}^{2+\frac{d_f}{2}(2-\tau)} \right. \\ &\times \left[ -2^{1+\frac{d_f}{2}(2-\tau)} \gamma \left( -2 - \frac{d_f}{2}(2-\tau), \frac{2\mathcal{D}A^{2/d_w}}{\|c\|^{2/d_f}} \right) \right. \\ &\left. \left. + \gamma \left( -2 - \frac{d_f}{2}(2-\tau), \frac{\mathcal{D}A^{2/d_w}}{\|c\|^{2/d_f}} \right) \right] A^{\frac{4+d_f(2-\tau)}{d_w}} \right\}. \end{aligned} \quad (20)$$

In eqn (18) we might set the lower limit of the integral to zero,  $\|c\| = 0$ , as the integral converges. We however find that taking into account the existence of the smallest cluster size  $\|c\|$  is necessary to grasp the numerical results below. When fitting eqn (19) and (20) to the simulation data with  $\|c\| = 0$ , the remaining two free parameters  $h$  and  $D$  were found to be insufficient to provide sufficiently good descriptions for  $\langle \overline{\delta c^2(\Delta)} \rangle$  and  $\langle \overline{\delta c^2(\Delta)} \rangle^2$ . Once a smallest cluster size is considered (we here choose the physical value  $\|c\| = 1$ )  $h$  and  $D$  can be optimised simultaneously to achieve a good fit to the simulations data.

Eqn (19) and (20) deserve two pertinent remarks. First, it is seen that when  $\mathcal{D}A^{2/d_w} \gg \|c\|^{2/d_f}$  in the argument of the incomplete gamma function  $\gamma$ , then the quantities  $\langle \overline{\delta c^2(\Delta)} \rangle$  and  $\langle \overline{\delta c^2(\Delta)} \rangle^2$  grow as a power of  $\Delta$ . Within the same limit, division of  $\langle \overline{\delta c^2(\Delta)} \rangle^2$  by  $\langle \overline{\delta c^2(\Delta)} \rangle$  yields an exponent for  $\Delta$  which is twice the gap exponent  $1/d_w$ , predicted by dynamical scaling theory.<sup>8,64</sup> In particular, both  $\langle \overline{\delta c^2(\Delta)} \rangle$  and  $\langle \overline{\delta c^2(\Delta)} \rangle^2$  are independent of the measurement time  $T$ . This is due to the averaging over all same-sized open clusters, as already alluded to above. To justify the validity of these scaling relations,  $D$  and  $h$  were optimised simultaneously for the two equations to achieve the best fit to the simulations results, represented by the dotted line in Fig. 2. The qualitative match between results (19) and (20) with the simulation results in Fig. 2 is quite good, given the conjectural arguments above.

The normalised variance of  $\langle \overline{\delta c^2(\Delta)} \rangle$  for an ensemble of finite size open clusters is given by

$$\text{EB}(\Delta) = \frac{\left( \langle \overline{\delta c^2(\Delta)} \rangle^2 \right) - \left( \langle \overline{\delta c^2(\Delta)} \rangle \right)^2}{\left( \langle \overline{\delta c^2(\Delta)} \rangle \right)^2} \geq 0, \quad (21)$$

which is a measure to quantify the amplitude fluctuations of individual results for the TAMSD at a given lag time  $\Delta$ . We emphasise that in this expression for EB no  $T$ -dependence remains due to the anisotropy average over finite-sized open clusters, as discussed above. Apart from the disorder average  $\langle \overline{\delta c^2(\Delta)} \rangle$  the quantity (21) has a similar structure as the ergodicity

breaking parameter introduced and studied in ref. 24, 25, 34, 44 and 65.

Substituting expressions (19) and (20) into eqn (21) we arrive at an analytical expression for EB. This expression contains a large number of cross-correlation terms such that we restrict ourselves to the limiting behaviour in the case  $\mathcal{D}A^{2/d_w} \gg \|c\|^{2/d_f}$  in which the incomplete gamma functions reduce to complete gamma functions. We then find that

$$\text{EB} \approx AA^{d_f(\tau-2)/d_w} - 1, \quad (22)$$

where  $A$  is a constant. The same result yields from eqn (18) by setting the lower integral limit to zero. Employing the hyper-scaling relation between  $d_f$  and  $\tau = d/d_f + 1$  where  $d$  is the embedding Euclidean dimension,<sup>9</sup> the above expression can be written exclusively in terms of  $d_f$  and  $d$ . Interestingly, the resulting form

$$\text{EB} \approx AA^{(d-d_f)/d_w} - 1, \quad (23)$$

has the same exponent of  $\Delta$  as the form for the parameter  $S$  proposed by Meroz *et al.*<sup>49,50</sup> to distinguish non-ergodic processes from ergodic ones. The difference is that here the ensemble is constituted by a cluster ensemble of different sizes, in contrast to the case addressed in ref. 49 and 50 where only incipient infinite clusters were considered.

The analytical solution (21) for EB with the fit parameters from Fig. 2 is plotted as function of lag time  $\Delta$  in Fig. 3 along with the results of our Monte Carlo simulations. The match is indeed rather good. What is clear from the double logarithmic plot in Fig. 3 is that for the displayed lag time values we see a crossover to the long- $\Delta$  scaling. The intermediate scaling at shorter  $\Delta$  has a steeper slope.

Another interesting observation is that the exponent of the lag time  $\Delta$  in eqn (19) can be rewritten in terms of the spectral dimension  $d_s = 2d_f/d_w$ .<sup>8,66</sup> Recalling the hyperscaling relation stated earlier between  $d_f$  and the Fisher exponent  $\tau$ , the expression of the disorder averaged TAMSD of eqn (19) can be rewritten as

$$\begin{aligned} \langle \overline{\delta c^2(\Delta)} \rangle &= (\tau - 2) \|c\|^{\tau-2} \left[ -2h^2 \|c\|^{2d_f+2-\tau} - d_f h^2 \mathcal{D}^{d_f/2} \right. \\ &\times \left. \gamma \left( \frac{d_f}{2}, \frac{\mathcal{D}A^{2/d_w}}{\|c\|^{2/d_f}} \right) A^{d_s/2} \right]. \end{aligned} \quad (24)$$

We emphasise that regardless of the type of the underlying lattice, in two dimensions and for long lag times,  $\Delta \rightarrow \infty$ , the disorder averaged TAMSD grows as  $\Delta^{d_s/2}$ . This sole dependence on the spectral dimension  $d_s$  is a consequence of the two-dimensional embedding.

### III. Discussion

We studied the amplitude fluctuations of the TAMSD typically measured in single particle tracking experiments or simulations for diffusion processes on a square percolation network at criticality. In particular we took all clusters of the network into account, not solely the incipient infinite cluster. Based on the conjectural analogy of this process with an Ornstein-Uhlenbeck

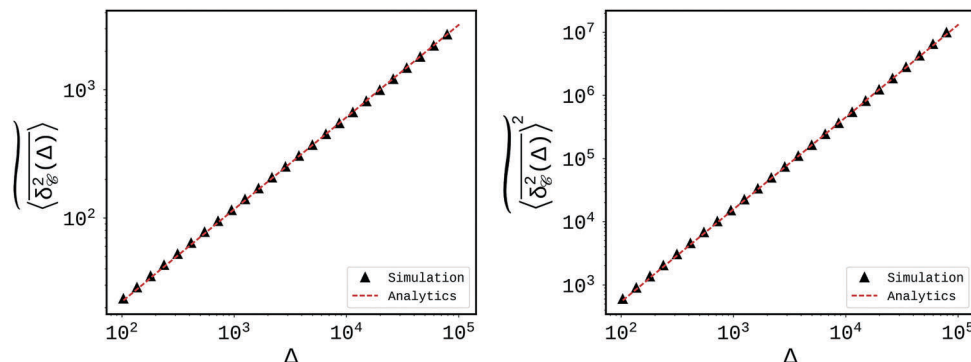


Fig. 2  $\langle \delta c^2(\Delta) \rangle$  (left) and  $\langle \delta c^2(\Delta) \rangle^2$  (right) versus  $\Delta$ . Dashed lines indicate the theoretical expressions (19) and (20). The simulation time was  $T = 10^6$ . The ensemble consists of  $5 \times 10^2$  lattices of size  $4096 \times 4096$ , on each lattice 50 random walks were simulated with  $D = 0.827$  and  $h = 0.375$ .

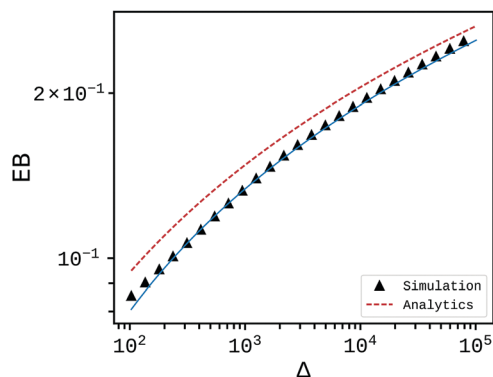


Fig. 3 Ergodicity breaking parameter EB versus lag time  $\Delta$ . The red dashed line represents eqn (21) based on results (19) and (20). The values of the adjustable parameters are  $D = 0.827$  and  $h = 0.375$ , the fit values being taken from Fig. 2. The blue full line is the scaling form of EB given by result (22) with the fitted value  $A = 0.98$ . The ensemble in the simulations consists of  $5 \times 10^2$  lattices, where on each 50 random walks were simulated.

process whose known results were rescaled in time we obtained the MSD and TAMSD for the diffusion on the ensemble of percolation clusters, under non-equilibrium initial conditions. The latter are appropriate for many single particle experiments and simulations, in which a tracer is put at a specific place on the percolation network initially. The results based on the analogy with the Ornstein-Uhlenbeck process were shown to be fully consistent with our simulations. Moreover, the expected analytical short and long time behaviours were recovered from the resulting expressions. In addition, it was shown that averaging over the anisotropy of clusters with a specific size yields an expression for the TAMSD which in this anisotropy-averaged sense is independent of the measurement time  $T$ . This consequently yielded a result for the normalised variance for the TAMSD, the ergodicity breaking parameter, which is independent of  $T$ , as well.

Let us briefly dwell on the connection with our earlier result. Thus, in ref. 51 we empirically suggested from simulation results that EB decays algebraically in  $T$  towards a residual value  $EB_\infty$  in the form

$$EB(\Delta) = k \left( \frac{\Delta}{T} \right)^g + EB_\infty(\Delta), \quad (25)$$

where  $k$  is a constant and  $g$  a scaling exponent, whose value for the square lattice was estimated to be 0.8. The constant  $EB_\infty$  was found to be an increasing function of the lag time  $\Delta$  and the percolation density  $p$ , as well as to acquire a non-zero value when  $p$  approaches the critical value  $p_c$ .<sup>51</sup> This form was proposed based on earlier analytical results for other stochastic processes such as Brownian motion, fractional Brownian motion, scaled Brownian motion, and continuous time random walks:<sup>25,34,67-70</sup> there EB decays as a power of  $T$ , with different scaling exponents, and, in some cases, attains a residual value. Here we demonstrate that the  $T$  dependence vanishes after taking the anisotropy average corresponding to an equilibrium initial condition, for which the dynamics is stationary. Due to computational limitations, however, it is impossible to sample all cluster configurations of the same size by means of Monte Carlo simulations. For instance, even for a small cluster of size 24 there are  $10^3$  configurations.<sup>71</sup> This is the reason why in our simulations we could observe a  $T$  dependence of EB, albeit this dependence is rather weak. This fact is illustrated in Fig. 4 which demonstrates that EB remains practically constant when  $T$  varies from  $10^4$  to  $10^6$ .

It will be interesting to extend the current study to other types of lattices and dimensions. For lattices embedded in two dimensions we would expect that the results obtained here can be transferred to other cases such as the triangular lattice. In higher dimensions it will have to be seen whether the residual, asymptotic value of EB is still relevant, and how the lag time scaling of the different averages of the TAMSD is modified.

As we discussed in the introduction, percolative systems are used as models for the study of protein diffusion in the chromatin of living cells or in the cellular cytoplasm.<sup>18,20</sup> Here the percolation network models areas of the cell that are inaccessible due to molecular crowding. Following recent simulation studies, in particular, in two spatial dimensions demonstrate that in crowded environments the size of the tracer particle itself may renormalise the accessible space.<sup>72</sup> Such effects may be included in more realistic percolation simulations. Moreover, it was shown that essential features of two-dimensional membrane systems consisting of small lipid molecules and large proteins, both mobile, can be mimicked by a static excluded volume system,<sup>73</sup> thus rendering static

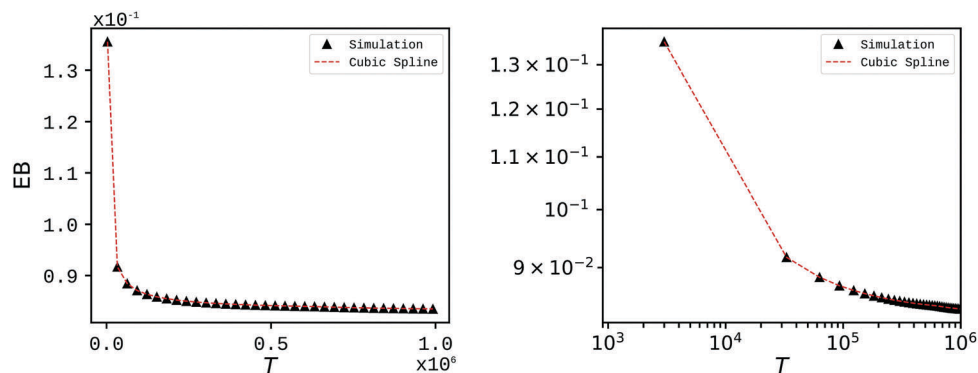


Fig. 4 EB versus  $T$  at  $\Delta = 10^2$ . The number of lattices in the ensemble is  $10^3$  on each of which  $2 \times 10^2$  random walks were simulated. Note the slight changes in EB while  $T$  varies between  $10^4$  to  $10^6$ .

approaches such as the percolation network applicable also to intrinsically dynamic systems.

Concluding, we are convinced that our results will be of interest not only to the further understanding of dynamics on percolation networks but of special relevance for the interpretation of single particle tracking experiments. In realistic situations one does not always have the flexibility to measure systems under equilibrium initial conditions, and averages of dynamic quantities are affected by inherent disorder in the system. Here our results of physical observables such as the MSD and the amplitude variations expressed in terms of the ergodicity breaking parameter will be easy to implement in data analysis. A particularly relevant area of current research is the single particle tracking of channel proteins in the membranes of living biological cells for which random fractal patterns have been unveiled from the trajectories.<sup>74,75</sup> This behaviour was associated with the self-similar compartmentalisation of the cortical actin meshwork.<sup>76</sup> Similarly relevant will be single particle tracking studies in the nucleus of living cells.<sup>18</sup>

## IV. Methods

### A. Simulation Scheme

The simulations were carried out on a square lattice, and the nearest neighbours of each site were identified by the von Neumann neighbourhood. The size of the lattice was set to  $4096 \times 4096$ , unless otherwise specified, when the size is set to  $1024 \times 1024$ . Each cell of the lattice is then attributed to be occupied with the percolation probability  $p$  or is left vacant otherwise. For the square lattice the critical percolation density  $p_c$  is not known analytically but it is, by the means of simulations, confirmed that  $p_c = 0.407254$  (note that vacant sites are of interest here).<sup>8,9</sup> In the simulations carried out here we used  $p_c = 0.4$ .

The initial position of the random walker is located at the centre of the lattice, which may belong to an open cluster or it is an occupied site. In the latter case, the nearest vacant site is chosen as the initial position. Therefore whether a random walker parachutes onto a finite size open cluster or onto an incipient

infinite cluster, is random and the associated probability related to the given cluster size  $\|C\|$ . For an illustration of such clusters see Fig. 1. The simulation time  $T$  is set to  $10^6$ . It is variable only when the dependence of the variance of the disorder averaged TAMSD on  $T$  is analysed, when it varies from  $10^4$  to  $10^6$ . The minimum lag time is  $\Delta = 10^2$  to guarantee that the topology of the underlying open clusters are sufficiently sampled.

The fractal dimension  $d_f$  was estimated as follows. An ensemble of  $7 \times 10^2$  incipient infinite clusters are analysed. It is clear that it is not readily observable whether the centre of the lattice belongs to a finite size cluster or to the incipient infinite cluster. Therefore to identify the open clusters and sieve the incipient infinite ones in a lattice realisation, the Hoshen–Kopelman algorithm is used.<sup>77</sup> Afterwards, the box counting method was used to estimate their fractal dimension  $d_f$ .<sup>78</sup> On average its corresponding value was found to be  $d_f = 1.9 \pm 0.1$ , which compares favourably with the predicted value  $d_f = 91/48 \approx 1.90$ . Yet it should be understood that every cluster has its own fractal dimension due to the unique anisotropy and inhomogeneity of the topology. The same applies to the random walk dimension  $d_w$ . To estimate  $d_w$  eqn (1) was used to extract the anomalous diffusion exponent  $\alpha$  for the incipient infinite clusters, and it was estimated as  $2.7 \pm 0.1$ , compared to the known value 2.87. The Fisher exponent  $\tau$  of the cluster size distribution at  $p_c$  is set to  $2.03 \pm 0.01$  based on earlier analyses on the distribution of finite size open clusters.<sup>51</sup> Again, this compares well with the literature value of  $\tau = 187/91 \approx 2.05$ .

**Simulation validation of phenomenological approach.** To verify the validity of eqn (5), (6), (10a) and (10b), analyses were performed on some finite size open clusters. Here for instance, a sample open cluster of size 793 on a lattice of size  $1024 \times 1024$  is demonstrated, see Fig. 1. Two initial conditions were considered: (i) the random walker was fixed to the centre of the underlying lattice at (512, 512), or (ii) the initial position was randomly chosen to be any site within the finite cluster. In total  $8 \times 10^3$  random walks were simulated and the result is shown in Fig. 5. In the left panel, corresponding to the fixed initial position, we note the gap of width  $R_g^2$  between the MSD and the TAMSD. This is the immediate consequence of how these

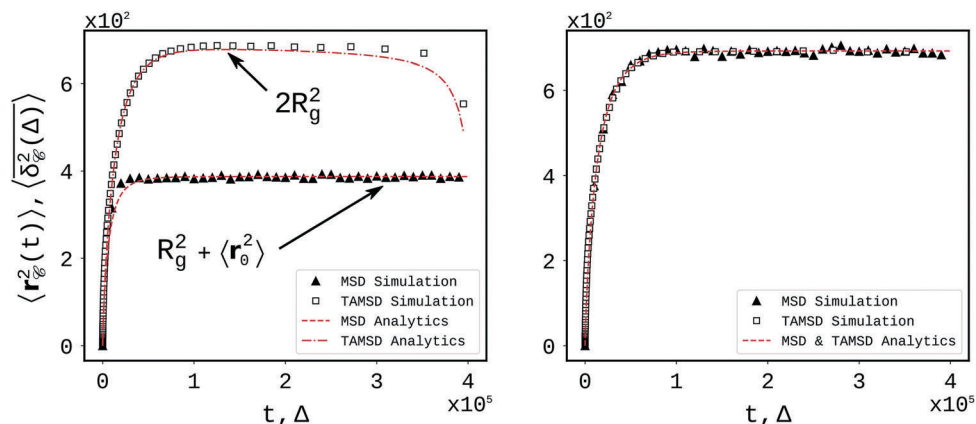


Fig. 5 MSD and TAMSD for fixed initial position (left) and arbitrary initial position (right) on a finite cluster of size 793.  $8 \times 10^3$  random walks were simulated. The x and y axes components of the co-ordinate of the centre of mass were found to be 513.74 and 518.20, respectively.  $R_g^2$  was measured to be 346.33.

quantities are defined in eqn (2) and (3); this is a well known disadvantage of these definitions for the stationary state of a diffusion process, see, for instance, ref. 25 and 79. In contrast, in the right panel, where the initial position was chosen arbitrarily, both reach the same asymptote, namely  $2R_g^2$ . In the procedure  $d_f \approx 1.60$  was estimated by the box counting method; the values  $d_w \approx 2.44$ ,  $D \approx 0.27$ , and  $h \approx 0.29$  were determined by best fit with the analytical expressions.

**Anisotropy average over same-sized open clusters.** To demonstrate that  $\langle \mathbf{r}_0^2 \rangle$ , once averaged over the anisotropy of clusters of the same size, is simply  $R_g^2$ , an analytical proof for the case of clusters of size three is provided here. There are two classes of clusters with the size three which are presented in Fig. 6. Note that clusters formed by applying the symmetry groups of the square lattice again belong to these two classes. Define these two classes with  $[-]$  and  $[\_L]$  (the upper row and the lower row in Fig. 6, respectively).

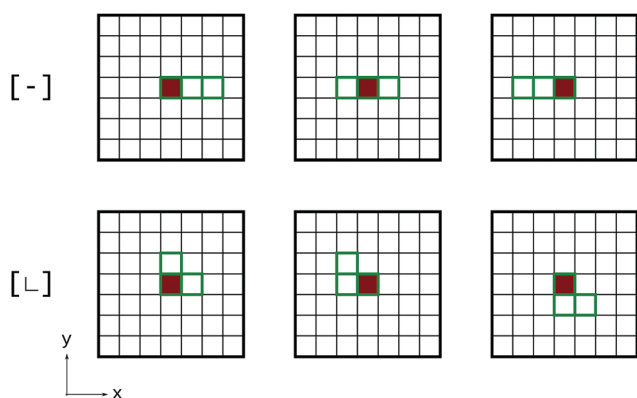


Fig. 6 Two classes of clusters of size three with their different sites positioned at the centre of the lattice. Other clusters which are formed by applying the symmetry groups of the square lattice are equivalent to these two. The x and y axes show the positive direction of the Cartesian co-ordinate, and the red square cell is the centre of the lattice located at (0, 0).

Consider the class  $[-]$ , then the following are the calculated values  $\langle \mathbf{r}_0^2 \rangle$  and  $R_g^2$  for the three possible configurations that appear at the centre of the lattice presented on the leftmost, middle, and rightmost panels of the first row of Fig. 6:

$$\left. \begin{aligned} \langle \mathbf{r}_0^2 \rangle &= (0 - 1)^2 = 1 \\ R_g^2 &= \frac{1}{3}[(0 - 1)^2 + (1 - 1)^2 + (2 - 1)^2] = \frac{2}{3} \end{aligned} \right\} \text{(Leftmost)} \quad (26)$$

$$\left. \begin{aligned} \langle \mathbf{r}_0^2 \rangle &= (0 - 0)^2 = 0 \\ R_g^2 &= \frac{1}{3}[(-1 - 0)^2 + (0 - 0)^2 + (1 - 0)^2] = \frac{2}{3} \end{aligned} \right\} \text{(Middle)} \quad (27)$$

$$\left. \begin{aligned} \langle \mathbf{r}_0^2 \rangle &= (-1 - 0)^2 = 1 \\ R_g^2 &= \frac{1}{3}[(-2 + 1)^2 + (-1 + 1)^2 + (0 + 1)^2] = \frac{2}{3} \end{aligned} \right\} \text{(Rightmost)} \quad (28)$$

Then the anisotropy average over  $\langle \mathbf{r}_0^2 \rangle$  yields  $\frac{1 + 1 + 0}{3} = \frac{2}{3}$ ,

which is equal to  $R_g^2$ . The same applies to the  $[\_L]$  class. Therefore it is supported that in eqn (15b) the quantity  $\langle \mathbf{r}_0^2 \rangle$  is indeed equal to  $R_g^2$ , once averaged over the anisotropy. This should not be surprising since this average is equivalent to an average over different initial positions of the random walks. However, to prove this numerically is practically impossible. For instance among the 9780 lattice realisations only 4 clusters of size 100 were identified. Thus the ensemble of finite clusters with size ranging from 100 to 149 comprised altogether 75. Although the size of these clusters varies somewhat,  $\langle \delta_c^2(\Delta) \rangle$  maintains practically stationary property for this very ensemble. In Fig. 7 we depict  $\langle \delta_c^2(\Delta) \rangle$  of these clusters (grey lines). Alongside  $\langle \delta_c^2(\Delta) \rangle$  is shown (thick black line). Note that there

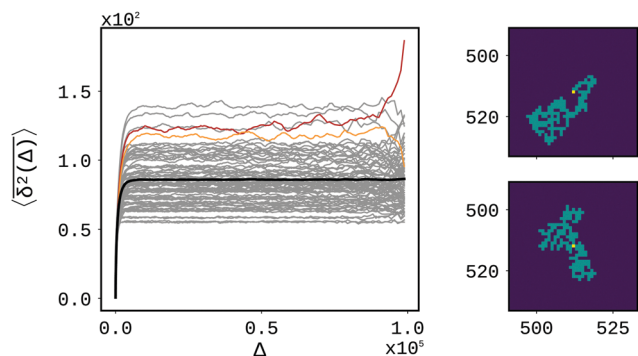


Fig. 7 TAMSD for a set of 75 clusters with size varying between 100 to 149 (grey). The tail of the TAMSD either ascends (red), corresponding to highly anisotropic cluster topologies depicted in the right panel top, or descends (yellow) which corresponds to more isotropic clusters depicted in the right panel bottom. The ensemble average of the TAMSDs are represented by the thick black line whose tail remains levelled. In the right panel the yellow dots represent the centre of the lattice at (512, 512) and the cyan colour depicts the finite cluster.

are two types of  $\langle \delta_c^2(\Delta) \rangle$  distinguished by their tail, which either ascends or descends (the red and yellow curves). The former corresponds to situations when the topological shape of the cluster is highly anisotropic (Fig. 7 right panel top) and consequently  $\langle r_0^2 \rangle > R_g^2$ . The latter case corresponds to situations when the finite cluster is distributed evenly around the centre of the lattice (Fig. 7 right panel bottom). Such cases imply that  $\langle r_0^2 \rangle < R_g^2$ . The tails of the resulted anisotropy averaged TAMSDs stays constant implying that the quantity (6) is indeed independent of  $T$ .

## Conflicts of interest

There are no conflicts to declare.

## Acknowledgements

A. V. C. and R. M. acknowledge support from Deutsche Forschungsgemeinschaft within project ME 1535/6-1 and ME 1535/7-1. J.-H. J. acknowledges financial support from NRF within project 2017R1C1B2007555. R. M. acknowledges support from the Foundation for Polish Science within an Alexander von Humboldt Polish Honorary Research Scholarship.

## References

- 1 B. B. Mandelbrot, *The Fractal Geometry of Nature*, W.H. Freeman, New York, 1977.
- 2 J. Feder, *Fractals*, Plenum Press, New York, NY, 1988.
- 3 H. Takayasu, *Fractals in the physical sciences*, John Wiley & Sons, Chichester, UK, 1992.
- 4 G. Cantor, Ueber unendliche, lineare Punktmannichfaltigkeiten, *Math. Ann.*, 1883, **21**, 545–591.
- 5 H. V. Koch, Sur une courbe continue sans tangente, obtenue par une construction géométrique élémentaire, *Ark. Mat., Astron. Fys.*, 1904, **1**, 681–704.
- 6 W. Sierpiński, Sur une courbe cantorienne dont tout point est un point de ramification, *Comptes Rendues Acad. Sci. Paris*, 1915, **160**, 302.
- 7 S. R. Broadbent and J. M. Hammersley, Percolation processes: I. Crystals and mazes, in *Mathematical Proceedings of the Cambridge Philosophical Society*, Cambridge University Press, Cambridge, 1957, vol. 53, pp. 629–641.
- 8 S. Havlin and D. Ben-Avraham, Diffusion in disordered media, *Adv. Phys.*, 1987, **36**, 695–798.
- 9 D. Stauffer and A. Aharony, *Introduction to Percolation Theory*, CRC Press, 1994.
- 10 P. G. de Gennes, La percolation: un concept unificateur, *La Recherche*, 1976, **7**, 919–927.
- 11 R. Metzler and J. Klafter, The random walk's guide to anomalous diffusion: a fractional dynamics approach, *Phys. Rep.*, 2000, **339**, 1.
- 12 A. Klemm, R. Kimmich and M. Weber, Flow through percolation clusters: NMR velocity mapping and numerical simulations study, *Phys. Rev. E: Stat., Nonlinear, Soft Matter Phys.*, 2001, **63**, 041514.
- 13 A. Klemm, R. Metzler and R. Kimmich, Diffusion on random site percolation clusters: theory and NMR microscopy experiments with model objects, *Phys. Rev. E: Stat., Nonlinear, Soft Matter Phys.*, 2002, **65**, 021112.
- 14 M. Sahimi, Fractal and superdiffusive transport and hydrodynamic dispersion in heterogeneous porous media, *Transp. Porous Media*, 1993, **13**, 3–40.
- 15 J.-P. Bouchaud and A. Georges, Anomalous diffusion in disordered media: statistical mechanisms, models and physical applications, *Phys. Rep.*, 1990, **195**, 127.
- 16 A. V. Weigel, *et al.*, Obstructed diffusion propagator analysis for single-particle tracking, *Phys. Rev. E: Stat., Nonlinear, Soft Matter Phys.*, 2012, **85**, 041924.
- 17 C. Loverdo, *et al.*, Quantifying hopping and jumping in facilitated diffusion of DNA-binding proteins, *Phys. Rev. Lett.*, 2009, **102**, 188101.
- 18 C. C. Fritsch and J. Langowski, Anomalous diffusion in the interphase cell nucleus: the effect of spatial correlations of chromatin, *J. Chem. Phys.*, 2010, **133**, 07B602.
- 19 M. Krasowska, A. Strzelewicz, A. Rybak, G. Dudek and M. Cieřła, Structure and transport properties of ethylcellulose membranes with different types and granulation of magnetic powder, *Phys. A*, 2016, **452**, 241–250.
- 20 M. J. Saxton, Anomalous diffusion due to obstacles: a Monte Carlo study, *Biophys. J.*, 1994, **66**, 394–401.
- 21 B. Oborny, V. Benedek, P. Englert, M. Gulyás and A. G. Hubai, The plant in the labyrinth: adaptive growth and branching in heterogeneous environments, *J. Theor. Biol.*, 2017, **412**, 146–153.
- 22 T. O. Richardson, K. Christensen, N. R. Franks, H. J. Jensen and A. B. Sendova-Franks, Ants in a labyrinth: a statistical mechanics approach to the division of labour, *PLoS One*, 2011, **6**, e18416.

- 23 M. J. Saxton, Lateral diffusion in an archipelago. the effect of mobile obstacles, *Biophys. J.*, 1987, **52**, 989–997.
- 24 E. Barkai, Y. Garini and R. Metzler, Strange Kinetics of Single Molecules in Living Cells, *Phys. Today*, 2012, **65**(8), 29.
- 25 R. Metzler, J.-H. Jeon, A. G. Cherstvy and E. Barkai, Anomalous diffusion models and their properties: non-stationarity, non-ergodicity, and ageing at the centenary of single particle tracking, *Phys. Chem. Chem. Phys.*, 2014, **16**, 24128–24164.
- 26 F. Höfling and T. Franosch, Anomalous transport in the crowded world of biological cells, *Rep. Prog. Phys.*, 2013, **76**, 046602.
- 27 R. Metzler, J.-H. Jeon and A. G. Cherstvy, Non-Brownian diffusion in lipid membranes: experiments and simulations, *Biochim. Biophys. Acta*, 1858, **2451**, 2016.
- 28 K. Nørregaard, R. Metzler, C. Ritter, K. Berg-Sørensen and L. Oddershede, Manipulation and motion of organelles and single molecules in living cells, *Chem. Rev.*, 2017, **117**, 4342.
- 29 J.-P. Bouchaud, Weak ergodicity breaking and aging in disordered systems, *J. Phys. I*, 1992, **2**, 1705.
- 30 H. Scher and E. W. Montroll, Anomalous transit-time dispersion in amorphous solids, *Phys. Rev. B: Condens. Matter Mater. Phys.*, 1975, **12**, 2455.
- 31 P. Massignan, *et al.*, Nonergodic subdiffusion from Brownian motion in an inhomogeneous medium, *Phys. Rev. Lett.*, 2014, **112**, 150603.
- 32 A. G. Cherstvy, A. V. Chechkin and R. Metzler, Particle invasion, survival, and non-ergodicity in 2D diffusion processes with space-dependent diffusivity, *Soft Matter*, 2014, **10**, 1591.
- 33 A. G. Cherstvy, A. V. Chechkin and R. Metzler, Anomalous diffusion and ergodicity breaking in heterogeneous diffusion processes, *New J. Phys.*, 2013, **15**, 083039.
- 34 Y. He, S. Burov, R. Metzler and E. Barkai, Random time-scale invariant diffusion and transport coefficients, *Phys. Rev. Lett.*, 2008, **101**, 058101.
- 35 A. Lubelski, I. M. Sokolov and J. Klafter, Nonergodicity mimics inhomogeneity in single particle tracking, *Phys. Rev. Lett.*, 2008, **100**, 250602.
- 36 S. Burov, R. Metzler and E. Barkai, Aging and non-ergodicity beyond the Khinchin theorem, *Proc. Natl. Acad. Sci. U. S. A.*, 2010, **107**, 13228.
- 37 J.-H. Jeon, V. Tejedor, S. Burov, E. Barkai, C. Selhuber-Unkel, K. Berg-Sørensen, L. Oddershede and R. Metzler, *In vivo* anomalous diffusion and weak ergodicity breaking of lipid granules, *Phys. Rev. Lett.*, 2011, **106**, 048103.
- 38 S. M. A. Tabei, *et al.*, Intracellular transport of insulin granules is a subordinated random walk, *Proc. Natl. Acad. Sci. U. S. A.*, 2013, **110**, 4911.
- 39 C. Manzo, *et al.*, Weak Ergodicity Breaking of Receptor Motion in Living Cells Stemming from Random Diffusivity, *Phys. Rev. X*, 2015, **5**, 011021.
- 40 J. H. P. Schulz, E. Barkai and R. Metzler, Aging renewal theory and application to random walks, *Phys. Rev. X*, 2014, **4**, 011028.
- 41 X. Hu, *et al.*, The dynamics of single protein molecules is non-equilibrium and self-similar over thirteen decades in time, *Nat. Phys.*, 2016, **12**, 171.
- 42 M. S. Song, H. C. Moon, J.-H. Jeon and H. Y. Park, Neuronal messenger ribonucleoprotein transport follows an ageing Lévy walk, *Nat. Commun.*, 2018, **9**, 344.
- 43 C. Monthus and J.-P. Bouchaud, Models of traps and glass phenomenology, *J. Phys. A*, 1996, **29**, 3847.
- 44 W. Deng and E. Barkai, Ergodic properties of fractional Brownian-Langevin motion, *Phys. Rev. E: Stat., Nonlinear, Soft Matter Phys.*, 2009, **79**, 011112.
- 45 J.-H. Jeon, N. Leijnse, L. Oddershede and R. Metzler, Anomalous diffusion and power-law relaxation in wormlike micellar solution, *New J. Phys.*, 2013, **15**, 045011.
- 46 I. Bronstein, *et al.*, Transient Anomalous Diffusion of Telomeres in the Nucleus of Mammalian Cells, *Phys. Rev. Lett.*, 2009, **103**, 018102.
- 47 M. Weiss, Single-particle tracking data reveal anticorrelated fractional Brownian motion in crowded fluids, *Phys. Rev. E: Stat., Nonlinear, Soft Matter Phys.*, 2013, **88**, 010101(R).
- 48 J. F. Revere, *et al.*, Superdiffusion dominates intracellular particle motion in the supercrowded space of pathogenic *Acanthamoeba castellanii*, *Sci. Rep.*, 2015, **5**, 11690.
- 49 Y. Meroz, I. M. Sokolov and J. Klafter, Test for determining a subdiffusive model in ergodic systems from single trajectories, *Phys. Rev. Lett.*, 2013, **110**, 090601.
- 50 Y. Meroz, I. M. Sokolov and J. Klafter, Subdiffusion of mixed origins: when ergodicity and nonergodicity coexist, *Phys. Rev. E: Stat., Nonlinear, Soft Matter Phys.*, 2010, **81**, 010101(R).
- 51 Y. Mardoukhi, J.-H. Jeon and R. Metzler, Geometry controlled anomalous diffusion in random fractal geometries: looking beyond the infinite cluster, *Phys. Chem. Chem. Phys.*, 2015, **17**, 30134–30147.
- 52 B. O’Shaughnessy and I. Procaccia, Analytical solutions for diffusion on fractal objects, *Phys. Rev. Lett.*, 1985, **54**, 455.
- 53 M. Giona and H. E. Roman, Fractional diffusion equation for transport phenomena in random-media, *Physica A*, 1992, **185**, 87.
- 54 R. Metzler, W. G. Glöckle and T. F. Nonnenmacher, Fractional model equation for anomalous diffusion, *Physica A*, 1994, **211**, 13.
- 55 B. D. Hughes, *Random Walks and Random Environments*, Clarendon Press Oxford, 1996, vol. 2.
- 56 D. Jacobs and H. Nakanishi, Autocorrelation functions for discrete random walks on disordered lattice, *Phys. Rev. A: At., Mol., Opt. Phys.*, 1990, **41**, 706.
- 57 C. D. Mitescu, H. Ottavi and J. Rousseny, Diffusion on percolation lattices: the labyrinthine ant, in *AIP Conference Proceedings*, AIP, 1978, vol. 40, pp. 377–381.
- 58 R. Pandey, Classical diffusion, drift, and trapping in random percolating systems, *Phys. Rev. B: Condens. Matter Mater. Phys.*, 1984, **30**, 489.
- 59 C. Fassnacht, *J. Undergrad. Res. Phys.*, 1983, **2**, 23.
- 60 C. D. Mitescu and J. Rosseny, Diffusion on percolation clusters. Percolation Structures and Processes, *Ann. Isr. Phys. Soc.*, 1983, **5**, 81–100.

- 61 J. Roussenq, PhD thesis, Université de Provence, Marseille, 1980.
- 62 G. E. Uhlenbeck and L. S. Ornstein, On the theory of the Brownian motion, *Phys. Rev.*, 1930, **36**, 823.
- 63 A. G. Cherstvy, Y. Mardoukhi, A. V. Chechkin and R. Metzler, under revision.
- 64 G. Grimmett, *Percolation*, Springer, 1999.
- 65 S. M. Rytov, Y. A. Kravtsov and V. I. Tatarskii, *Principles of Statistical Radiophysics: Correlation theory of random processes. Principles of Statistical Radiophysics*, Springer-Verlag, 1987.
- 66 S. Alexander and R. Orbach, Density of states on fractals: “fractons”, *J. Phys. (Paris), Lett.*, 1982, **43**, L625–L631.
- 67 M. Schwarzl, A. Godec and R. Metzler, Quantifying non-ergodicity of anomalous diffusion with higher order moments, *Sci. Rep.*, 2017, **7**, 3878.
- 68 H. Safdari, *et al.*, Quantifying the non-ergodicity of scaled Brownian motion, *J. Phys. A*, 2015, **48**, 375002.
- 69 A. Bodrova, *et al.*, Underdamped scaled Brownian motion: (non-)existence of the overdamped limit in anomalous diffusion, *Sci. Rep.*, 2016, **6**, 30520.
- 70 A. G. Cherstvy and R. Metzler, Ergodicity breaking, ageing, and confinement in generalized diffusion processes with position and time dependent diffusivity, *J. Stat. Mech.: Theory Exp.*, 2015, **2015**, P05010.
- 71 D. H. Redelmeier, Counting polyominoes: yet another attack, *Discrete Math.*, 1981, **36**, 191–203.
- 72 S. Ghosh, A. G. Cherstvy, D. Grebenkov and R. Metzler, Anomalous, non-Gaussian tracer diffusion in heterogeneously crowded environments, *New J. Phys.*, 2016, **18**, 013027.
- 73 J.-H. Jeon, M. Javanainen, H. Martinez-Seara, R. Metzler and I. Vattulainen, Protein crowding in lipid bilayers gives rise to non-Gaussian anomalous lateral diffusion of phospholipids and proteins, *Phys. Rev. X*, 2016, **6**, 021006.
- 74 A. V. Weigel, B. Simon, M. M. Tamkun and D. Krapf, Ergodic and nonergodic processes coexist in the plasma membrane as observed by single molecule tracking, *Proc. Natl. Acad. Sci. U. S. A.*, 2011, **108**, 6438.
- 75 D. Krapf, Mechanisms underlying anomalous diffusion in the plasma membrane, *Curr. Top. Membr.*, 2015, **75**, 167.
- 76 S. Sadegh, J. L. Higgins, P. C. Mannion, M. M. Tamkun and D. Krapf, Plasma membrane is compartmentalized by a self-similar cortical actin meshwork, *Phys. Rev. X*, 2017, **7**, 011031.
- 77 J. Hoshen and R. Kopelman, Percolation and cluster distribution. i. cluster multiple labeling technique and critical concentration algorithm, *Phys. Rev. B: Condens. Matter Mater. Phys.*, 1976, **14**, 3438.
- 78 K. Falconer, *Fractal geometry*, John Wiley & Sons, Chichester, UK, 1990.
- 79 J.-H. Jeon and R. Metzler, Inequivalence of time and ensemble averages in ergodic systems: exponential *versus* power-law relaxation in confinement, *Phys. Rev. E: Stat., Nonlinear, Soft Matter Phys.*, 2012, **85**, 021147.